iEnergy

ARTICLE

https://doi.org/10.23919/IEN.2022.0031

Design of the flame retardant form-stable composite phase change materials for battery thermal management system

Xinxi Li[1], Zixin Wu[1], Qiqiu Huang[1], Canbing Li[2] ✉, Yang Jin[3], Guoqing Zhang[1], Wensheng Yang[1], Jian Deng[1], Kang Xiong[2] and Yuhang Wu[2]

ABSTRACT

Phase change materials have attracted significant attention owing to their promising applications in many aspects. However, it is seriously restricted by some drawbacks such as obvious leakage, relatively low thermal conductivity, and easily flame properties. Herein, a novel flame retardant form-stable composite phase change material (CPCM) with polyethylene glycol/epoxy resin/expanded graphite/magnesium hydroxide/zinc hydroxide (PEG/ER/EG/MH/ZH) has been successfully prepared and utilized in the battery module. The addition of MH and ZH (MH:ZH = 1:2) as flame retardant additions can not only greatly improve the flame retardant effect but also maintain the physical and mechanical properties of the polymer. Further, the EG (5%) can provide the graphitization degree of residual char which is beneficial to building a more protective barrier. This designation of CPCM can exhibit leakage-proof, high thermal conductivity (increasing 400%–500%) and prominent flammable retardant performance. Especially at 3C discharge rate, the maximum temperature is controlled below 54.2 °C and the temperature difference is maintained within 2.2 °C in the battery module, which presents a superior thermal management effect. This work suggests an efficient and feasible approach toward exploiting a multifunctional phase change material for thermal management systems for electric vehicles and energy storage fields.

KEYWORDS

Battery thermal safety, thermal management system, composite phase change material, form stable, flame retardant, controlling strategy.

Electric vehicle (EV) plays a key role in reducing carbon emission. Lithium-ion batteries (LIB) with high energy density and specific energy have been widely utilized in various vehicles and energy storage devices[1,2]. Although the capacity, cycling life, and charging rate of LIB have been greatly improved, thermal safety issues still need to be addressed[3–5]. Owing to LIB with a narrow temperature range and voltage window, the heat generated by LIB could not be dissipated timely and is still a serious risk. It would activate the self-sustained cascading exothermic reactions when the temperature of batteries surpassed the threshold and lead to thermal runaway continually[6–8]. Thus, to release the heat generated by batteries timely, an efficient battery thermal management system (BTMS) is vital for the safety of EV. According to the transferring heat media, the BTMS has been mainly categorized into air cooling[9,10], liquid cooling[11,12], and phase change material (PCM) cooling[13–15] systems. Air cooling is simple and economical, but it has a low convective heat transfer coefficient. The liquid cooling system is efficient, which can not only enhance the energy consumption but also have the potential for thermal hazards, facing challenges such as extra equipment, liquid leakage, and high cost. Thus, developing an advanced BTMS is imperative to satisfy the requirements of battery thermal safety.

Phase change material (PCM) as a passive cooling system has been utilized in the battery module, which can absorb or release large amounts of heat while its temperature keeps constant during the melting or solidifying process, and it has great potential application in different fields as a latent heat storage technique[16–18]. Polyethylene glycol (PEG)[19,20] as a typical phase change material has many permits such as high enthalpy, consistent melting behavior, good chemical and thermal stability, low vapor pressure, and so on. Although the PEG has been utilized in different fields, it still contains several shortcomings such as low thermal conductivity, liquid leakage, and phase separation. The inherent low thermal conductivity can limit the heat transfer within PCMs and lead to the reduction of thermal diffusion rate. A general method to address this problem is to incorporate metal-, carbon- or ceramic-based high-thermal-conductivity additives into the PCM matrix[21–26]. Among these additions, expanded graphite (EG) has been tremendously utilized to improve thermal conductivity[27,28]. Compared with the problem of dissipating heat capacity, liquid leakage appeared as a more troublesome agenda that is worth concentrating on because the fluid PCMs could lead to contamination, corrosion, and even bring about short circuits of equipment. Considering these reasons, numerous investigators have endeavored to address this issue, and epoxy resin (ER)[29] as an important thermosetting polymer can effectively improve the molding ability of PCM and solve the leakage problem, owing to excellent chemical stability, adhesive strength, and dielectric properties. However, the ER mainly composed of carbon, hydrogen, and oxygen exhibits extremely flammable properties. Thus, it is very necessary to explore a flame retardant addition to improve the thermal stability of composite phase change material (CPCM).

Generally, adding flame retardant additives to shape-stable

[1]School of Materials and Energy, Guangdong University of Technology, Guangzhou 51006, China; [2]Department of Electrical Engineering, Shanghai Jiao Tong University, Shanghai 200240, China; [3]School of Electrical Engineering, Zhengzhou University, Zhengzhou 450001, China
Address correspondence to Canbing Li, licanbing@sjtu.edu.cn

PCMs is the most common method to improve their thermal stability and suppress their flammability[30]. Compared with organic flame retardants, inorganic flame retardants mainly include inorganic phosphates, nitrogen-containing materials, and inorganic metal hydroxide flame retardants[31–35]. Metal hydroxide flame retardants have been considered to be a promising flame retardant additive owing to their excellent flame retardancy and environmental friendliness[36]. As a halogen-free flame retardant material, metal hydroxide can not only produce an endothermic reaction during combustion and decrease the surface temperature of the polymer but also release water molecules and dilute the concentrated combustible gas. In addition, the metal oxides can form a protective layer on the surface to cut off the heat source at the point of combustion, which will further inhibit the release of flammable gases and decrease the effects of flame and smoke[37]. Among these halogen-free flame retardants, magnesium hydroxide (MH) acts as a reinforcing filler, which significantly improves the mechanical properties of the matrix and plays an important role in suppressing flame retardants and gas phase fumes, which also dilutes the flammable pyrolysis products and acts as heat resistance to promote carbonization.[38,39] However, the MH has inherently inefficient, which could be formed char layer with too thin, brittle, and full of cracks characteristics after combustion. Thus, it needs to improve the flame retardant further. Considering the CPCM added with zinc hydroxide (ZH) can contribute to forming a compactly protective barrier with a high graphitization degree during the combustion of polymers, which can also benefit the conversion of MH-based polymeric materials to graphite materials, so it is promising to add ZH to reduce the damage of MH on the mechanical property of epoxy (EP). However, there is no research about the various metal hydroxide added in CPCM to improve the flame retardant effect, which would contribute to forming a strong protective barrier with a high condensing degree during the combustion of CPCM.

Until now, the effective method to synthesize flame retardant from stable CPCM is still lacking and needs to explore further. In this study, a novel flame-retardant form stable composite phase change material based on PEG/EG/ER/MH/ZH was successfully prepared and utilized in the battery module. The addition of two metal hydroxide can not only improve the flame retardant effect but also enhance the thermal stability of CPCM. Besides, the EG is also benefited to build an effective protective barrier. The thermophysical properties and flame retardancy of the polymer were studied from the macroscopic and microscopic levels. Besides, the battery module with different CPCMs have been assembled and measured, the results reveal that the PCM adding with MH and ZH (PEMZ) displays a prominent thermal management effect for battery module owing to synergistical effect, which indicates this designing CPCM has a prominent prospect in energy storage and thermal management fields.

1 Battery thermal management in EVs

1.1 CPCM for passive thermal management of battery pack

As the power source of electric vehicles, the battery pack plays an important role in sustaining endurance mileage and power available capacity. The battery pack is usually installed between the front and rear axles in the chassis position of EV, and its weight can reach about 900 kg, as shown in Figure 1(a). This design of battery pack in the chassis center can cause low gravity, which is conducive to enhance the high-speed stability of the vehicle. Figure 1(b) indicates that the battery pack almost occupies the entire chassis of the vehicle, but it is not as the main body of bearing force to affect its performance. The pack is protected by stiffeners and a stressed frame, greatly reducing the risk of explosion in the event of a collision. In addition, as an important protection measure to improve the thermal safety of the battery pack, the battery thermal management system can not only interact with the battery pack, auxiliary cooling heat exchanger, circulating water pump, and other devices in the electric vehicle, but also provide necessary thermal management effect for the battery pack (Figure 1(c)). Air cooling

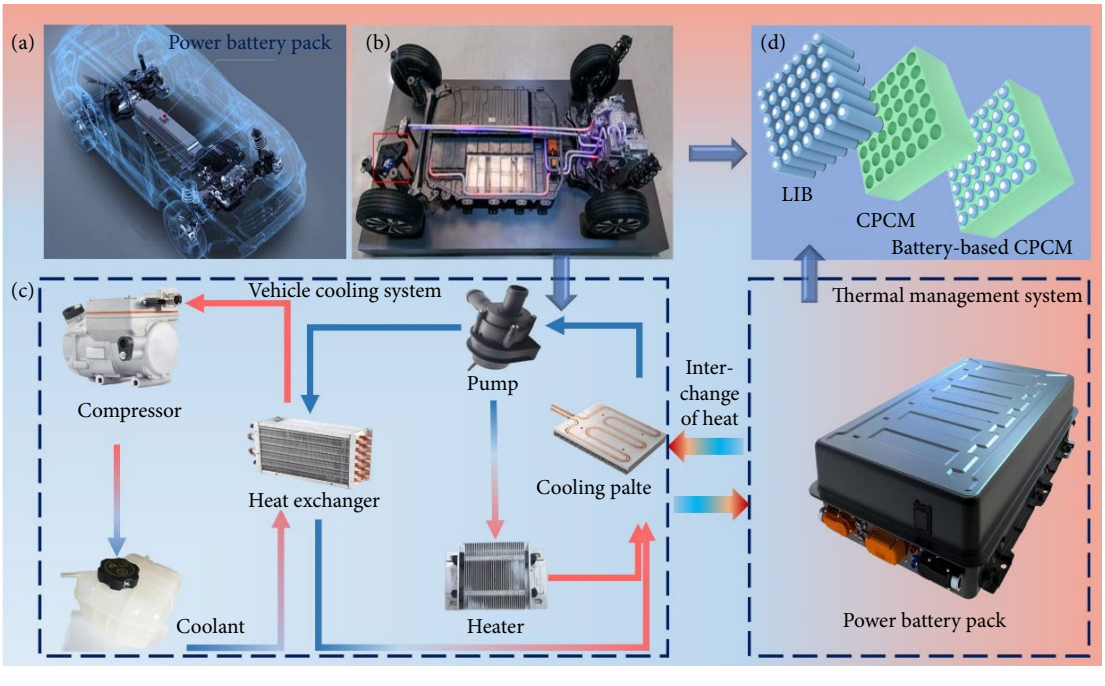

Fig. 1 **(a)** The battery pack installed in the chassis of EV; **(b)** the battery pack between the front and rear axles; **(c)** BTMS interacting with other dissipating heat devices in EV; **(d)** CPCM as passive cooling approach in the battery pack.

is simple and economical, but it exhibits a low convective heat transfer coefficient, and a liquid cooling system is relatively high dissipating heat efficiency, which can not only enhance the energy consumption but also have the potential for thermal hazards, facing challenges such as extra equipment, liquid leakage, and high cost. Compared with those, as depicted in Figure 1(d), the CPCM as passive cooling approach has great potential in the battery pack, which can provide excellent control temperature and uniform temperature effect.

1.2 Preparation of the flame retardant CPCM

Analyzing the schematic of the fabrication process of flame retardant form-stable CPCM (FR-CPCM), as displayed in Figure 2(a), indicates that adding an appropriate amount of MZ and HZ into the system can uniformly distribute among the PEG, which could be combined with EG to form stable three-dimensional structure to strengthen the structure of CPCM. Besides, the ER mixed with these materials can provide crosslink and firm structure to prevent leakage, it can significantly inhibit the shape change and improve the thermal stability of CPCM. The materials utilized in this experiment have been provided in Section SI 1.1 which is in the Supplementary Information (SI) of the online version of this article. The FR-CPCM was prepared by a traditional physical mixing method, which was shown in Figure 2(b). First, the polyethylene glycol 2000 (PEG) was melted in an oil bath at 80 °C. After PEG was melted completely, MH and ZH were added into the bath and stirred with a magnetic stirrer (400 rad·min^{-1}) for 30 min. Subsequently, the pre-weighed EG was added to the oil bath. Until EG was fully mixed, ER was poured into the bath under magnetic stirring at 400 rad·min^{-1} and stirred for 60 min to allow it to mix evenly with the PCM. And then, the curing agent was poured into the mixture and stirred for 5 min, allowing the ER to form a strong supporting skeleton. The liquid phase CPCM was also flowed into a special acrylic mold with six battery shape acrylic sticks for curing for 24 h. Herein, the ZH and MH flame retardants have been designed and added into PEG/EG/ER composite material with different proportions, as listed in Table 1. When the CPCM module had been prepared, six batteries in parallel were assembled into the module.

1.3 Battery thermal management system testing

The chemical characterization and thermophysical properties of CPCMs are described in Section SI 1.2 in the SI. The relevant instruments of the shape stability, leakage measurement, and flame retardant properties of CPCM are also displayed in the Figure S1. The thermal control performance of FR-CPCM-based battery thermal management systems (BTMS) was tested in this section. To compare the battery thermal management characteristics of

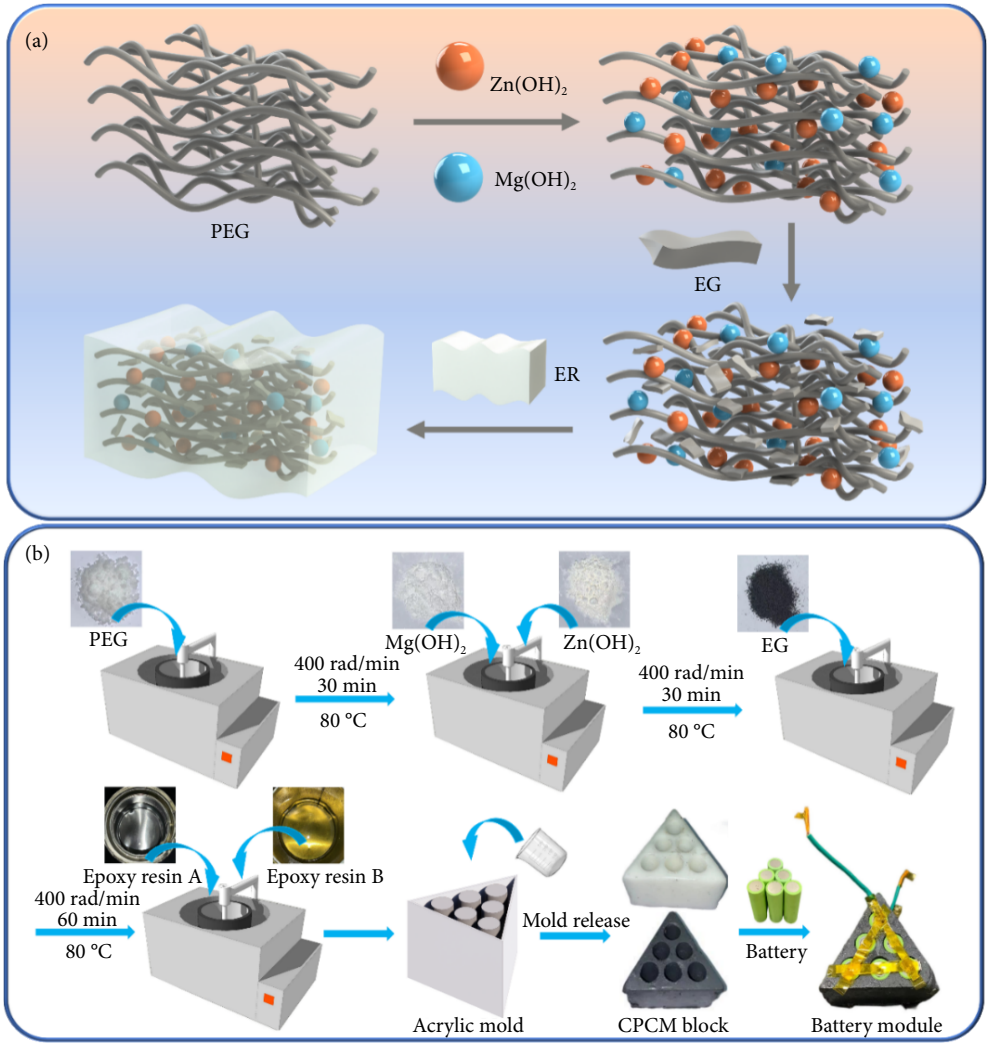

Fig. 2 **(a)** The fabrication schematic of FR-CPCM; **(b)** the preparation process of FR-CPCM and assembled into battery module.

Table 1 The CPCM with different proportions of components including MH and ZH flame retardants

Sample	PEG	EG	ER	$Mg(OH)_2$	$Zn(OH)_2$
Pure PEG	100%	—	—	—	—
PE	65%	5%	30%	—	—
PEM	65%	5%	15%	15%	—
PEM_2Z_1	65%	5%	15%	10%	5%
PEM_1Z_2	65%	5%	15%	5%	10%
PEZ	65%	5%	15%	—	15%

different CPCMs, pure PEG, PE, and PEM_1Z_2 were selected, and corresponding battery modules were built. As shown in Figure 3, the battery temperature measurement system was set up, and the CPCMs can be characterized through various methods. The battery thermal management testing platform included a battery testing system, connecting to a computer with a testing system software and a temperature collector, and the detailed test platform of the battery module was displayed in Figure S1 in the SI. Besides, thermocouples were attached to the center of each battery and connected to the temperature collector. The battery module was composed of six 18650-type batteries (Li-ion battery, Li Shen Battery Co., Ltd., China) connecting in parallel. The parameters of the battery and the battery module are listed in Table S1 in the SI.

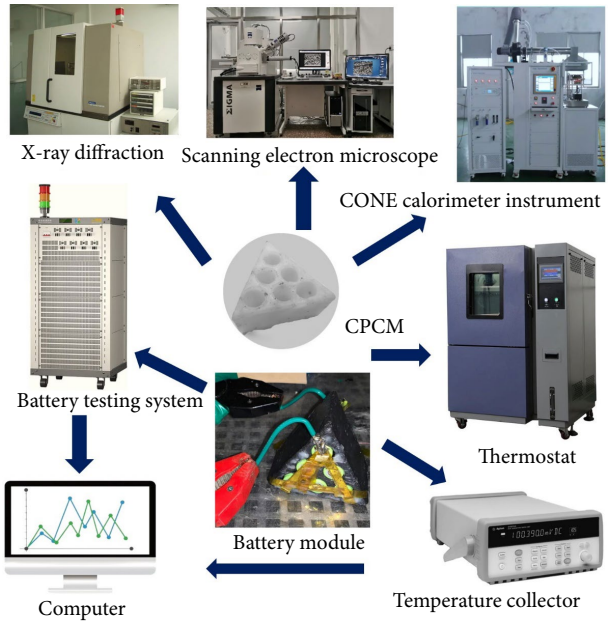

Fig. 3 The test platform of the battery module and the main measuring equipment of CPCM.

2 The analysis of chemical characterization and thermophysical properties

2.1 The characteristics of chemical composition

In order to study the chemical composition changes of CPCM after complete combustion, the X-ray diffraction (XRD) curves of different CPCMs were compared and analyzed, as shown in Figures 4(a) and 4(b). The XRD curves of different CPCMs in Figure 4(a) show that the PE has sharp peaks at 19.63° and 23.81°, which conform to the typical peaks of PEG and the peak at 26.64° (002) corresponded to the characteristic peak of EG (Figure S2 in the SI). Towards the PEM, it reveals that six peaks in its XRD curve correspond to the characteristic peaks of MH, as depicted in Figure 4(a). When both MH and ZH flame retardants were added to CPCM, the XRD curves of PEM_1Z_2 and PEM_2Z_1 are very similar, and the characteristic peaks corresponded to MZ and ZH. This indicated that no chemical reaction occurred during the preparation of FR-CPCM, and both ZH and MH can mix well with CPCM and retain their original flame retardant properties. After combustion, the XRD curves of FR-CPCM showed obvious changes. Figures 4(b) indicates that all CPCMs still have a peak at 26.64° (002) which corresponds to typical peaks of EG, indicating that EG had no chemical changes during combustion. The characteristic peaks of PEG disappeared, which reflected that PEG had been completely decomposed and volatilized during combustion. In the FR-CPCM combustion process, MH decomposed at high temperatures and generated the water vapor and MgO, as described in Section SI 1.4 in the SI. According to the analysis of XRD patterns after complete combustion, it can be concluded that ZH and MH had thermal decomposition reactions during complete combustion, and two kinds of refractory materials ZnO and MgO were generated. At the same time, PEG and ER were completely burned out, while EG maintained the original crystal structure.

2.2 The thermophysical properties of CPCM

The latent heat value of CPCM is an important parameter affecting its thermal management characteristics. Thus, the differential scanning calorimetry (DSC) curves of different CPCMs before combustion were compared, as shown in Figure 4(c). The pure PEG has a latent heat value of 99.05 $J \cdot g^{-1}$ and its phase transition temperature is 45 °C. The phase transition temperatures of different FR-CPCMs are maintained at 42–44 °C, and the main reason is that EG can greatly improve the thermal conductivity of CPCM and allow PEG to absorb heat quickly. Besides, with the addition of other materials, the corresponding latent heat value of CPCM obviously decreases. It should be contributed that the EG with abundant pore structures could have a strong adsorption and fixation effect on PEG molecules, it effectively limited the free movement of the PEG molecular chain in the phase transition process of CPCM, resulting in a decrease in latent heat. With the increase of flame retardant addition, the latent heat value is further reduced because large numbers of flame retardant particles were added which limited the molecular thermal motion during the PEG phase transition process, thus reducing its latent heat. The latent heat values of different CPCMs before and after combustion are listed in Table S2 in the SI, which indicates that the latent heat value of CPCM decreased sharply after combustion. The latent heat values of PEM_1Z_2 and PEM_2Z_1 are still higher than PE, PEM, and PEZ after combustion, and the main reason is that ZH and MH decomposed in the combustion process can produce water

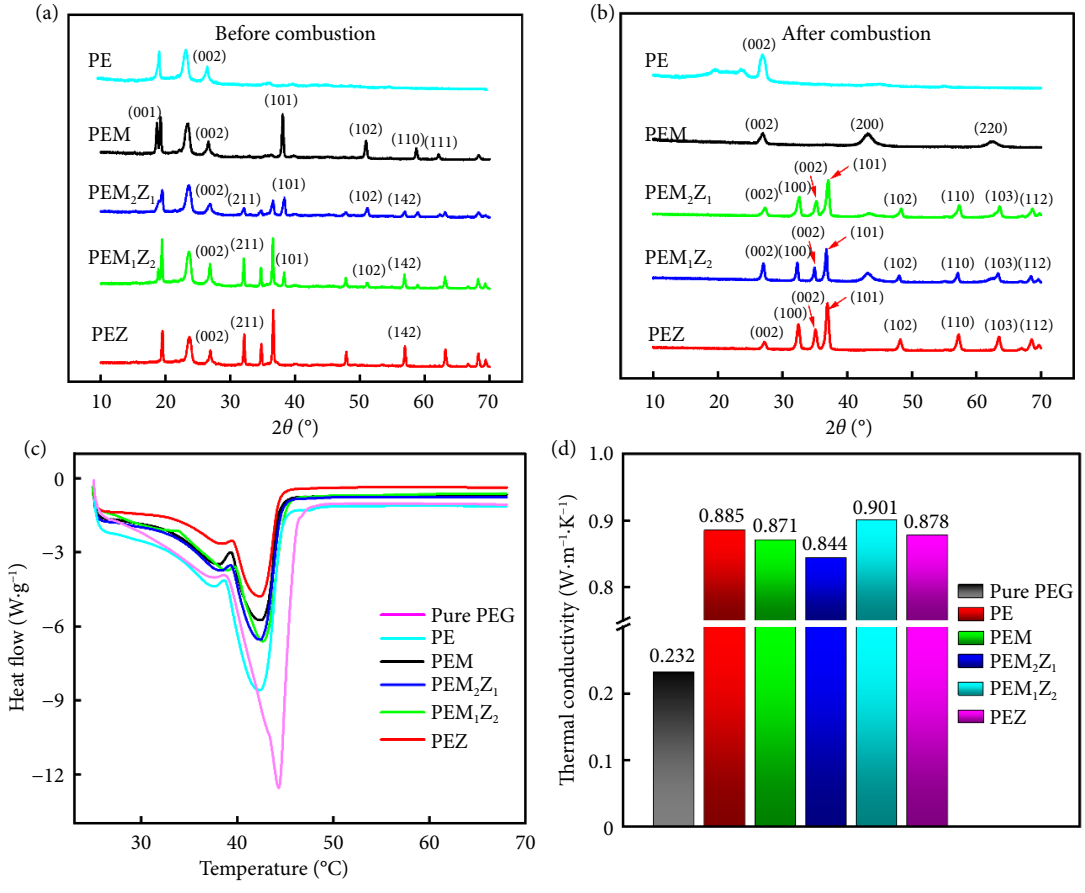

Fig. 4 The characteristics of different of CPCM samples. (a) XRD curves before combustion, **(b)** XRD curves after combustion, **(c)** DSC curves, and **(d)** thermal conductivity.

vapor to dilute oxygen and generated ZnO and MgO refractories uniformly, which effectively prevent the entry of oxygen and heat.

The thermal conductivity of different CPCMs is shown in Figure 4(d), which indicates that the thermal conductivity of pure PEG is only 0.232 $W \cdot m^{-1} \cdot K^{-1}$, accompanied by the addition of EG, the thermal conductivity of each CPCM is significantly improved. The thermal conductivity of PEM_1Z_2 reaches 0.901 $W \cdot m^{-1} \cdot K^{-1}$, which is 3.88 times higher than that of pure PEG. The main reason is that worm-like EG had high thermal conductivity and form an excellent thermal conductivity path, thus effectively enhancing the thermal conductivity of CPCM. Besides, MH and ZH particles can also be filled with the CPCM, which could increase the crosslink of the thermal conductivity network, thus improving the thermal conductivity of CPCM to a certain degree.

2.3 The thermal gravimetric analyzer and the shape stability capacity of different CPCMs

To further analyze the thermal stability of CPCM at high temperatures, the thermal gravimetric analyzer (TGA) curves of different CPCMs are analyzed, as shown in Figure 5(a), and the correlative data are listed in Table S3 in the SI. It can be observed that the pyrolysis of each sample exhibited only one stage and the degradation curves are similar. When the temperature exceeded 340 °C, the CPCM become to decompose and the mass decreased rapidly, and this stage is mainly the pyrolysis of PEG and ER. With the ZH flame retardants addition, the initial temperature of the degradation platform gradually increased. The addition of flame retardants can alleviate the decomposition of CPCM and improve the stability of CPCM. The char residue of pure PEG and PE at 600 °C is only 7.23% and 11.45%, respectively. However, the CPCMs with flame retardant additions can surpass 22%, the PEM_1Z_2 exhibit the optimum residual mass of 26.69%, and it is ascribed that the mass contained the carbon and oxides (MgO and ZnO) residues. It is contributed to the synergistic flame retardant effect of ZH and MH, which could produce a large amount of water vapor after decomposition. Besides, the generated oxides have strong heat resistance and are uniformly distributed in the carbon layer, thus forming a heat barrier and stable carbon layer. Thus, these results indicate that MH and ZH with a 1:2 ratio can obtain optimum thermal stability.

In addition, the shape stability affected the lifespan and thermodynamic property of the CPCM, particularly applied in the battery module. The quality maintenance rate curves of different CPCMs are shown in Figure 5(b), and the samples were photographed to record the leaking degree shown in Figure 5(c). It reveals that the pure PEG block melted quickly and entirely after 15 min. In the first 30 min, these CPCMs totally exhibited leakage of varying degrees, among which PE had serious leakage of PEG during phase transformation, and its quality assurance rate decreases to 97.5% after 30 min. With the extension of the heating time, the leakage mass is decreased and the curve tends to be flat which meant the speed of the leakage was slowed down. It can be observed that CPCM with the ER and EG quality maintained above 96.5% after 180 min, which indicates that ER and EG could significantly improve the leakage performance of CPCM. By comparison with the leakage of PEM, PEZ, and PEM_2Z_1 under heating continually conditions in Figure S3 in the SI, these results show that PEM_1Z_2 exhibits excellent antileakage performance with a

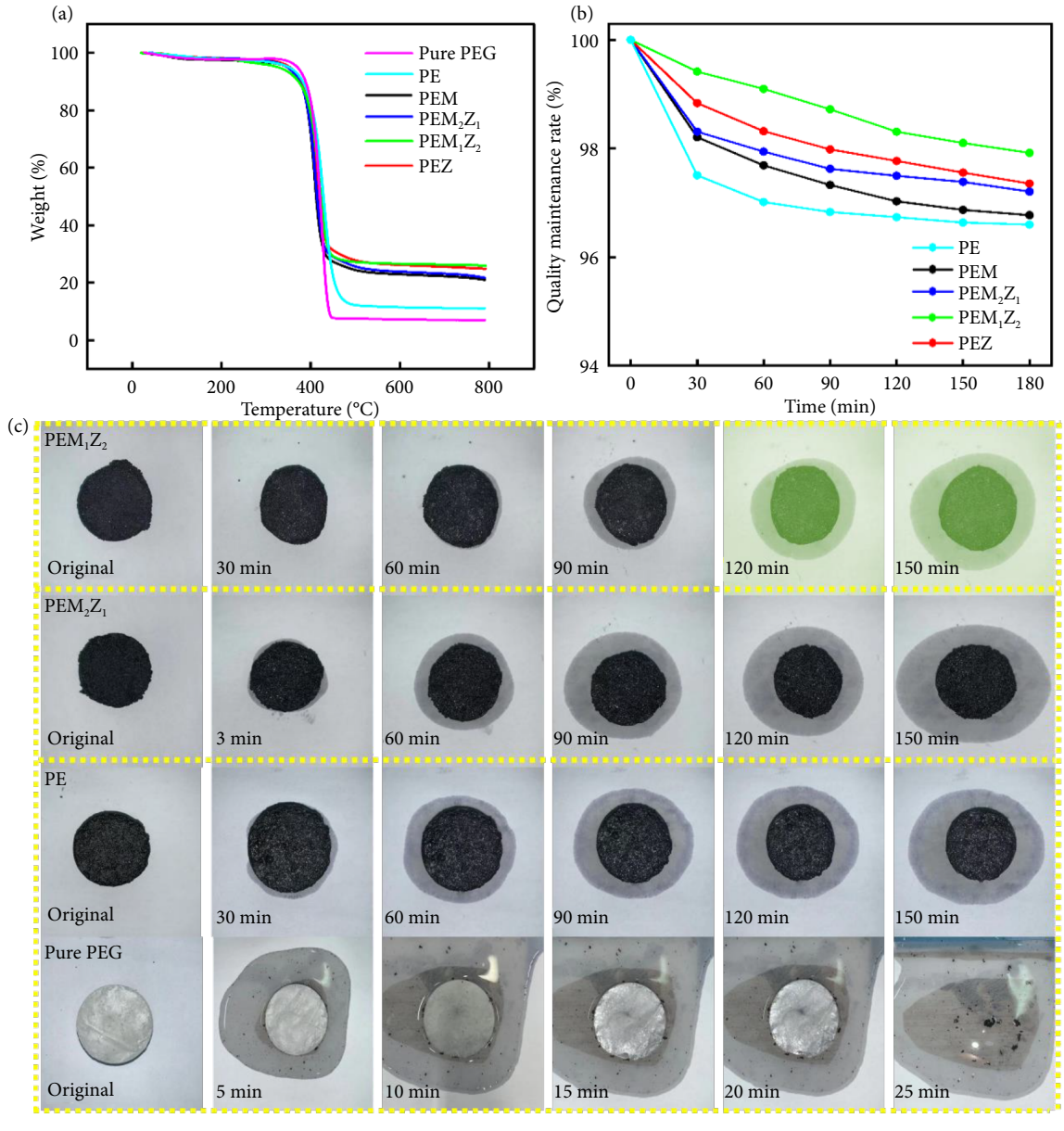

Fig. 5 The characteristics of different CPCM samples. **(a)** TGA analysis, **(b)** quality maintenance rates, and **(c)** leakage measurements.

quality maintenance rate of 98.1%. The main reason is that ER with a cross-linked structure can coat the PEG to prevent the leakage of CPCM, and the abundant three-site pore structure with EG can effectively adsorb PEG. Additionally, ZH and MH as suitable proportion distributed uniformly in EG sheets can further enhance the adsorption capacity of EG.

3 The flame retardant performance discussion of different CPCMs

In order to analyze the combustion degree and flame retardant performances of different CPCMs intuitively, the different strips of these samples are utilized to measure the vertical combustion and limiting oxygen index (LOI) measurement. Besides, the cone calorimeter test is one of the effective methods utilized to evaluate the flame retardant performance of different CPCMs. The combustion of CPCM is accompanied by the generation of a large amount of heat and smoke, so the flame retardant characteristics of CPCM are comprehensively evaluated by analyzing heat release rate (HRR), total heat release (THR), smoke production rate (SPR), and total smoke production (TSP).

3.1 Vertical combustion and LOI measurement

The UL-94 grade, LOI value, and total duration of residual flames (TDORF) results of each CPCM are shown in Table 2. The UL-94 grade of PE without flame retardant just reached V-2, and the LOI value is 18.6%, which reflects that the PE could be easily burned and EG has a weak flame retardant effect. When MH and ZH were added separately, UL-94 grades of PEM and PEZ both got to V-1, and the total duration of residual flames was reduced to 13.2 and 12.4 s, respectively. It illustrates that the addition of ZH and MH singly improves the flame retardant ability of CPCM. However, owing to the different decomposition temperatures of ZH and MH, it could not play a flame retardant role in a wide temperature range. At the same time, the heat-resistant oxides could not distribute uniformly on the surface of the carbon layer, which cause the failure to protect the carbon layer, resulting in cracks of the carbon layer under the impact of the flame and eventually

Table 2 LOI and UL-94 results of different CPCMs

Sample	LOI (%)	UL-94	TDORF[a] (s)
PE	18.6	V-2	30.3
PEM	20.4	V-1	13.2
PEM_2Z_1	25.6	V-0	10.1
PEM_1Z_2	29.1	V-0	8.5
PEZ	21.7	V-1	12.4

[a]Total duration of residual flames.

leading to the penetration of oxygen and heat. When MH and ZH are added together as synergistic flame retardants, it indicates that the UL-94 level of PEM_1Z_2 and PEM_2Z_1 are reached to V-0 level. The results show that the synergistic effect of ZH and MH exhibit a good flame retardant performance, which is better than that of a single flame retardant. However, the LOI values of PEM_1Z_2 and PEM_2Z_1 are 29.1% and 25.6%, respectively, which indicates the PEM_1Z_2 can exhibit excellent flame retardant effect when MH and ZH added with suitable proportion. The main reason is that ZnO particles generated abundantly during the combusting process, which can distribute on the surface of the carbon layer compactly and play synergistic effect with MgO. Thus, the PEM_1Z_2 can effectively prevent CPCM between the ignition of early stage and the reburn in later stage.

3.2 Cone calorimeter and char residue analysis

To observe the combustion degree and combusting process of FR-CPCM intuitively, various strips of samples are selected for the vertical combustion test as shown in Figures 6(a)–6(c). Pure PEG has rapidly melted and continues to fall and burn after flame heating, and a thin black carbon layer is generated on the surface. After flame heating for only 30 s, the remaining length of the pure PEG is only about 20% of the original length (see Figure 6(a)). The remaining length of PE is about 50%, as shown in Figure 6(b). With the addition of ZH and MH flame retardants, the retention rate has been greatly improved. As shown in Figure 6(c), the residual length of PEM_1Z_2 after ignition reaches about 90%. With the further increase in temperature, ZH presents to decompose and produce a large amount of water to cool down, dilute the oxygen on the spline surface and generate ZnO particles. ZnO particles are evenly distributed on the surface of the carbon layer and jointly protected the carbon layer and the internal substrate with MgO particles. Thus, PEM_1Z_2 displays the optimum flame retardant performance. In addition, the cone calorimeter test results of different samples are displayed in Table 3. In Figure 6(b), the peak heat release rate (PHRR) value of the PE without flame retardant reaches 759.2 $kW{\cdot}m^{-2}$ after ignition, indicating that PE is easy to burn. With the addition of flame retardant ZH, the PHRR value of PEZ with 722.2 $kW{\cdot}m^{-2}$ is not decreased greatly, indicating that the flame retardant effect is poor when ZH existed alone. The main reason is that the decomposition temperature of ZH is high, and ZH has not decomposed much at the initial combustion temperature. The addition of MH significantly reduced the PHRR value of PEM (577.1 $kW{\cdot}m^{-2}$), which decrease by 20.1%, indicating that the decomposition temperature of MH was lower than that of ZH. The PHRR value of PEM_1Z_2 and PEM_2Z_1 with ZH and MH composite decreased by 501.3 $kW{\cdot}m^{-2}$ and 518.2 $kW{\cdot}m^{-2}$, respectively. The results indicated that synergistic flame retardant of MH and ZH could reduce the maximum PHRR effectively. MH played the main flame retardant role in the early stage, and ZH played the leading flame retardant role as the combustion continued. Besides, Figure 6(e) recorded the total heat release (THR) values of different CPCMs, it reveals THR value decreased significantly when the MH and ZH were added. The THR value of PEM_1Z_2 is only 119.4 $MJ{\cdot}m^{-2}$, which reflects that PEM_1Z_2 has good flame retardancy.

Further, as shown in Figure 6(f), PE exhibits a fast smoke production rate (SPR), reaching 0.046 $m^2{\cdot}s^{-1}$. With the addition of ZH and MH, the smoke release rate gradually decreases, which is due to the formation of ZnO and MgO after the thermal decomposition of ZH and MH, and the isolation layer was formed on the surface of CPCM, which effectively slowed down the smoke release rate after combustion. Besides, EG formed a uniform and solid expanded carbon layer after combustion, and its porous and layered structures inhibit the formation of smoke. PEM_1Z_2 is the lowest SPR value with only 0.022 $m^2{\cdot}s^{-1}$. Besides, the total smoke production (TSP) curves of the total smoke emission of CPCM are shown in Figure 6(g), which reveals that the TSP values decrease to varying degrees accompanied by the additions of ZH and MH. The TSP of PEZ is 4.9 m^2, which is obviously lower than that of PEM is 5.8 m^2, indicating that ZH has a better smoke suppression effect. The reason is that ZnO generated by ZH could uniformly coat the surface of CPCM to form an isolation layer, preventing oxygen from penetrating into the interior, which plays an essential role in flame retardant and smoke suppression. Therefore, these results reveal that PEM_1Z_2 can display an excellent flame retardant effect, and the synergistic flame retardant effect of ZH and MH is better than those of single hydroxide.

3.3 The morphology of different samples and the mechanism of flame retardant

Figure 7 shows the images of CPCM after cone calorimeter combustion and the SEM of different samples before and after combustion. Initially, it indicates each CPCM forms carbon layers of different degrees after combustion, as shown in Figures 7(a)–7(a3). The reason is that EG has a unique worm-like structure, which can absorb a large amount of heat and form a protective layer to carry out the flame retardant function. It could be seen from Figures 7(b)–7(b3) that there are more voids and larger cracks on the surface of carbon residue, which was not conducive to the isolation of oxygen and heat transfer. After adding ZH and MH, the carbon layer becomes much more compact and stable due to the formation of ZnO and MgO after pyrolysis of ZH and MH in Figures 7(c)–7(c3), which are stable refractory materials that can effectively isolate oxygen and protect internal materials. As shown in Figures 7(d)–7(d3), white powder particles at the label are ZnO and MgO particles, which are evenly distributed in CPCM, effectively improving the flame retardant ability of CPCMs and preventing the release of air. In Figures 7(e)–7(e3), the single ZnO cannot form compact layer on the surface of CPCM, and it presents obviously cracks in the composite material. Thus, it can be induced that the carbon layers of PEM_1Z_2 after the combustion exhibit a better tightly distribution than other samples, and the main reason is that the ZnO depositing on the surface of the carbon layer abundantly can built an isolation layer, which could form heat insulation and fire resistance barriers with synergistic effect, thus preventing the exchange of material, heat, and oxygen, to display an optimum flame retardant effect.

Further, the schematic diagrams of the combustion process of different CPCMs are analyzed. As shown in Figure 8(a), pure PEG melted rapidly after ignition, and the flame increased with the melting PEG, which eventually led to the spread of the flame. As for PE, when cross-linked ER and worm-liked EG wrapped PEG effectively, the flow phenomenon of PE during combustion would be weakened, which was described in Figure 8(b). Heat and oxygen

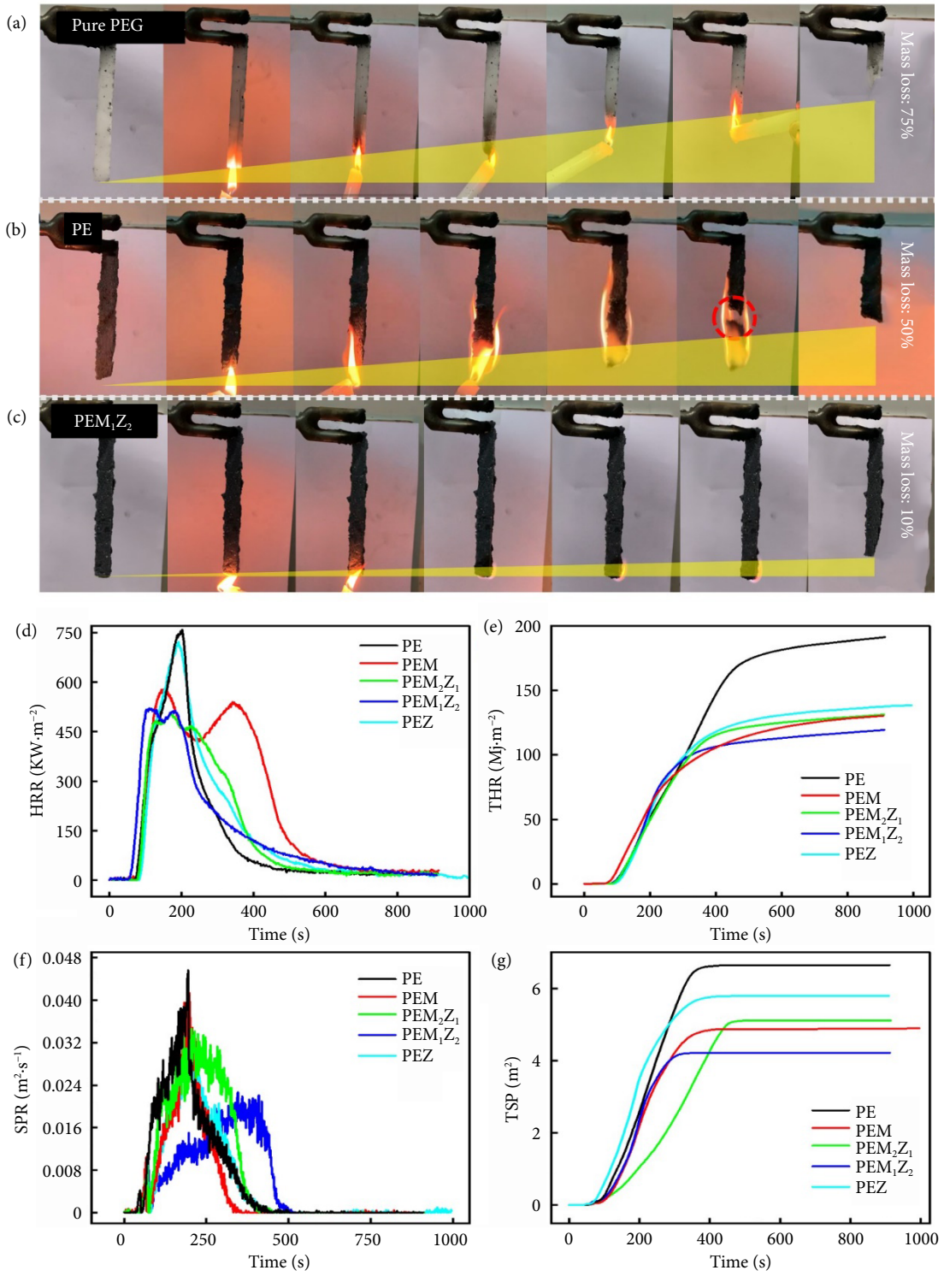

Fig. 6 Images of different CPCM vertical combustions. (a) Pure PEG, **(b)** PE, and **(c)** PEM_1Z_2. **Cone testing results of different CPCMs. (d)** Heat release rate (HRR), **(e)** total heat release (THR), **(f)** smoke production rate (SPR), and **(g)** total smoke production (TSP).

can enter the interior of the material from the gaps in the discontinuous EG carbon layer, delaying the cessation of the combustion process. When MH and ZH are added, MH and ZH particles can be evenly dispersed in CPCM. When FR-CPCM is burned at a high temperature, due to the low decomposition temperature of MH and ZH, which can decompose and form isolating heat layer and release water vapor, realizing the initial inhibition of flame retarding, as shown in Figure 8(c). In this process, the gas phase and solid phase can occur to play the flame retardant effect (Figure 8(d)). When the combustion process continued and the temperature is further increased. The former layer can obtain good fire resistance and it evenly distributes in the carbon layer, effectively isolating the heat and further strengthening the density of the carbon layer so that oxygen could not enter the interior, while the latter layer plays a role in dilution of oxygen. ZnO formed by combustion could form a more stable heat insulation

Table 3 The cone calorimeter test results of different samples

	TTI[a] (s)	PHRR (kW·m^{-2})	THR (MJ·m^{-2})	TSP (m^2·kg^{-1})
PE	203	759.2	191.4	6.6
PEM	153	577.1	130.8	5.8
PEM_2Z_1	121	518.2	131.2	5.1
PEM_1Z_2	162	501.3	119.4	4.1
PEZ	192	722.2	138.6	4.9

[a]TTI stands for the combustion time corresponding to the peak heat release rate.

and oxygen insulation layer at the bottom of the single MgO, which effectively fills the gap between MgO and achieved effective isolation of heat and oxygen. The synergistic effect of ZH and MH can also generate a carbon layer by CPCM during combustion, so the PEM_1Z_2 can exhibit an obvious and efficient effect in heat and oxygen insulation.

4 The thermal management effect of battery modules with different CPCMs

To verify the effectiveness of the prepared CPCM for BTMS, six 18650 lithium-ion batteries were paralleled into a battery module. Combined with the performance analysis of CPCM in Sections 4.1 and 4.2, pure PEG, PE, and PEM_1Z_2 were selected and built up for corresponding BTMS, and their heat dissipation and temperature uniformity characteristics were tested and analyzed. The three modules were tested for 15 cycles of charge and discharge at different discharge rates (1C, 2C, and 3C), and the temperature of the battery module was monitored by T-type thermocouples. The results of temperature for each battery module are shown in Figure 9. According to Figure 9(a), the highest temperatures of pure PEG-Module at 1C and 2C discharge rates are 52.5 and 57.9 °C, respectively. When the discharge rate was 3C, the maximum temperature is over 65 °C. It could be seen from Figure 9(b) that the maximum temperature of PE-Module is 60.8 °C at the 3C discharge rate. The addition of EG improves the thermal conductivity of CPCM, which could effectively transfer the absorbed heat and avoid a large amount of heat accumulation. Finally, with the addition of flame retardant ZH and MH, the heat dissipation performance of the battery is further improved. As shown in Figure 9(c), the maximum temperature changes of PEM_1Z_2-Module at the rates of 1C, 2C, and 3C are 42.5, 48.6, and 54.8 °C, respectively. Meanwhile, the highest temperature is reduced by 19.4% compared with that of pure PEG-Module at the rate of 3C.

Besides, temperature consistency is also one of the important performances of BTMS. The temperature distributions of the battery module are closely related to the electrochemical performance, cycling life, and safety performance of the battery. As shown in Figure S4 in the SI, at 1C discharge rate, the maximum temperature difference among the three modules is totally small. When the discharge rate increased to 2C, the maximum temperature differences of pure PEG-Module, PE-Module, and PEM_1Z_2-Module are 1.92, 2.91, and 4.14 °C, respectively. When the discharge rate reached 3C, the maximum temperature difference of pure PEG-Module reaches 6.63 °C, but PEM_1Z_2-Module still maintains a low maximum temperature difference and is only 2.51 °C, which indicates that the temperature consistency of CPCM has been greatly improved with the addition of EG and flame retardants.

To further analyze the utility of CPCM in battery thermal management, 15 cycles of charge and discharge tests were performed on three battery modules. In the cycling process at 1C charge and discharge rate, the temperature differences of the three battery modules are relatively close, among which the temperature difference of the PEM_1Z_2-module is the smallest, which could basically maintain below 1.5 °C, as depicted in Figure 9(d). With the increase of discharge rate, the temperature difference of the battery module in the cycle test also increases, the temperature difference of pure PEG-Module raises to 4°C, and the temperature difference tends to rise with the accumulation of cycle times (Figure S5 in the

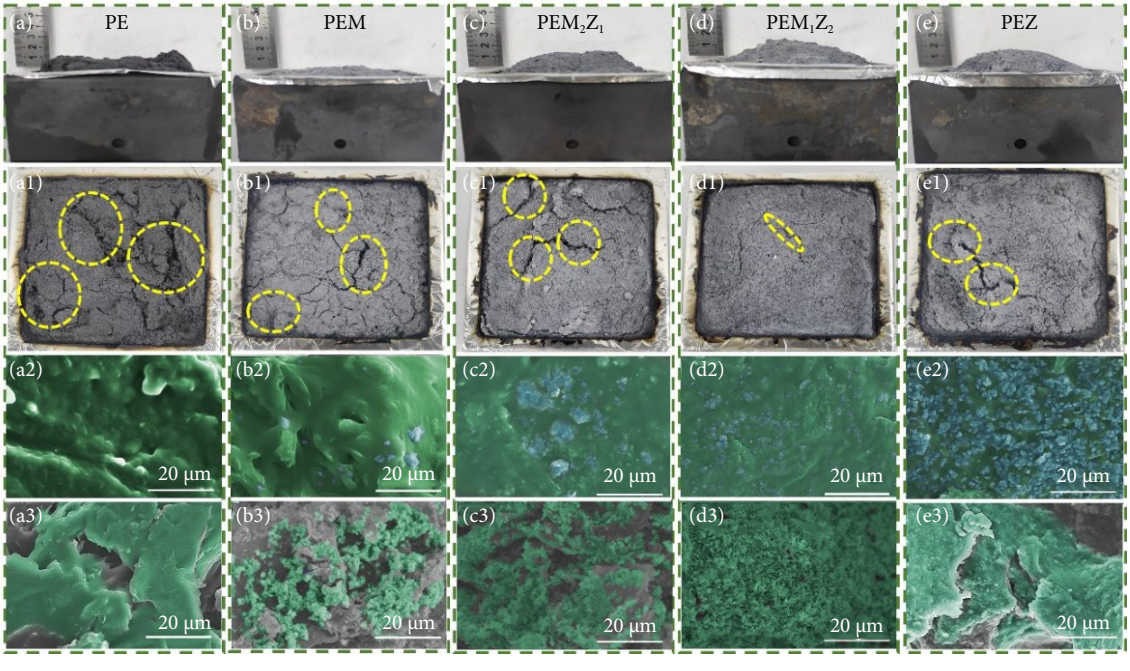

Fig. 7 Images of different CPCMs after cone tests. (a) PE, **(b)** PEM, **(c)** PEM_2Z_1, **(d)** PEM_1Z_2, and **(e)** PEZ. **The surface morphology of different CPCMs after combustion tests. (a1)** PE, **(b1)** PEM, **(c1)** PEM_2Z_1, **(d1)** PEM_1Z_2, and **(e1)** PEZ. **The SEM of different CPCMs before and after combustion. (a2–a3)** PE, **(b2–b3)** PEM, **(c2–c3)** PEM_2Z_1, **(d2–d3)** PEM_1Z_2, and **(e2–e3)** PEZ.

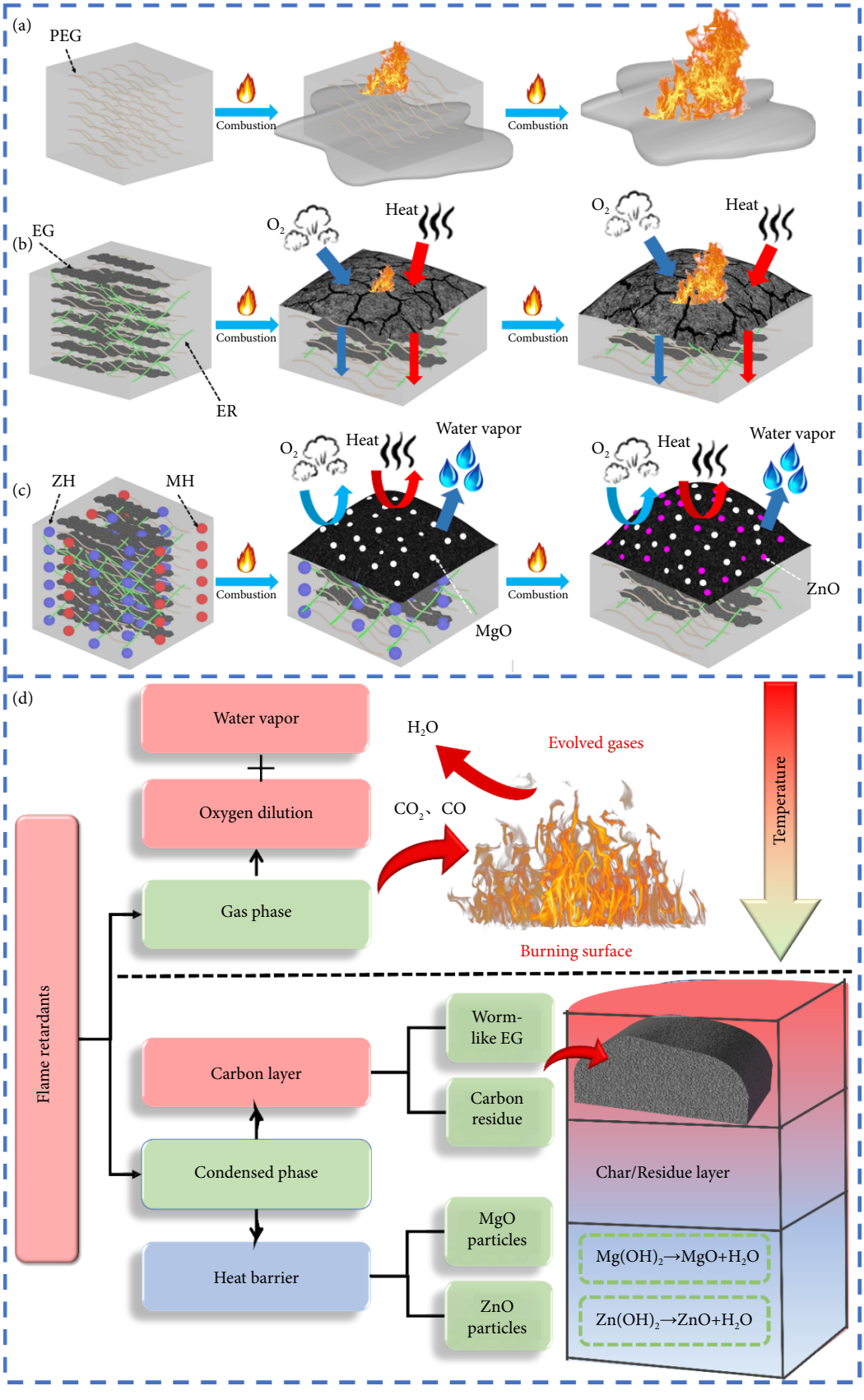

Fig. 8 **The flame retardant schematic of CPCM. (a)** Pure PEG, **(b)** PE, **(c)** PEM_1Z_2; **(d)** the diagram analysis between gas phase and condensed phase sections.

SI). As shown in Figure 9(e), the maximum temperature difference of pure PEG-module reaches 6.6 °C at a discharge rate of 3C. Excessive rising temperature has a strong destructive effect on the electrode material, diaphragm, and electrolyte of lithium-ion battery. Serious cases may cause a short circuit and cause thermal runaway accidents. Due to the higher thermal conductivity of PE,

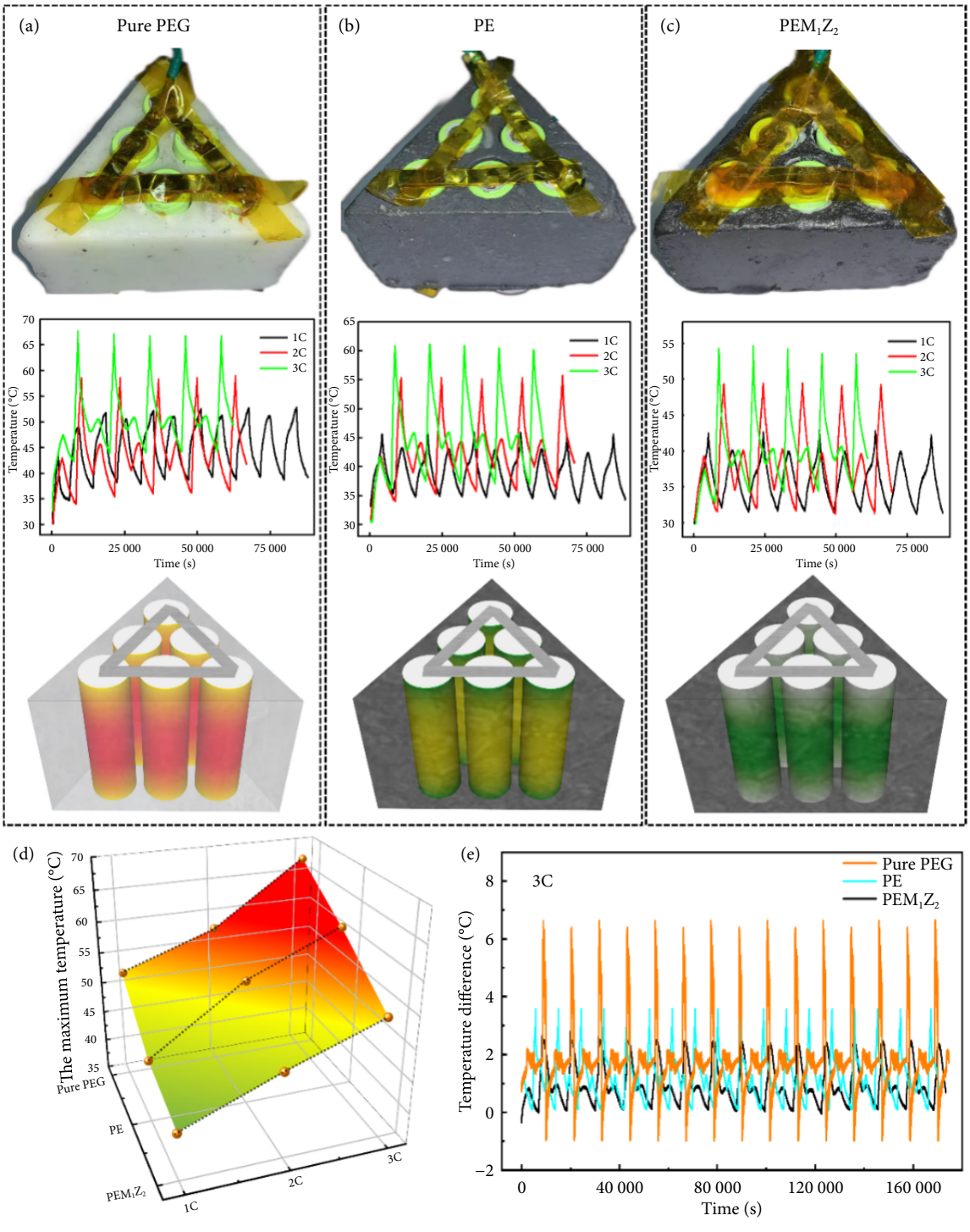

Fig. 9 The temperature of the battery module at different discharge rates (1C, 2C, and 3C). (a) Pure PEG-Module, **(b)** PE-Module, and **(c)** PEM_1Z_2-Module; **(d)** the maximum temperature difference of battery modules at different discharge rates; **(e)** the temperature difference change of battery modules at 3C discharge rate.

the temperature difference in the battery module drops to about 3.6 °C during the cycle charge and discharge test. Correspondingly, the PEM_1Z_2-Module presents the optimum temperature uniformity. The maximum temperature difference of the battery module can be maintained below 3 °C, which would effectively ensure the temperature consistency of the battery module.

5 Conclusions

PCMs are a promising thermal storage medium in various aspects, but their low thermal conductivity and easily flammable property often limit their great application. Although several investigations focus on improving the thermal conductivity of these materials, still few research that concentrated on multifunction CPCM with flammable properties. In this study, a novel flame retardant forms stable CPCM has been successfully designed and prepared. The CPCM has been characterized thoroughly and utilized in the battery module. Besides, three different CPCMs are selected and utilized in the battery module, which aims to improve the thermal management effect. The results revealed that composite PCMs con-

taining the flame retardancy (MH:ZH = 1:2) can exhibit optimum high-quality carbon layer with a compact and homogeneous structure and obtain excellent flame retardant performance, it achieved the highest LOI value of 29.1%, and the total heat release value of 119.4 MJ·m^{-2}.

Compared with the pure PEG cooling systems, the composite flame retardant and form stable CPCM displays an optimum thermal management effect. At 3C discharge rate under 25 °C condition, the peak temperatures of module with pure PEG and PE decreased by 19.3% and 9.2%, respectively. And the peak temperature difference was kept within 2.2 °C. Even at 3C high discharge, the maximum temperature of PEM_1Z_2 was reduced by 19.3%, and the temperature differences were maintained at 2.2 °C. The investigations reveal that the battery module with PEM_1Z_2 plays an important role in decreasing the temperature and balancing the temperature difference, especially at a high discharge rate.

Considering the above analysis, it should be concluded that this designed CPCM with outstanding thermal properties can not only improve the thermal management effect for the battery module but also apply in potential various energy fields. This research provides a fundamental basis for designing CPCM property targets and can be a critical tool for researchers and practitioners in developing thermal storage materials and devices.

Acknowledegments

This work is supported by the Natural Science Foundation of Guangdong province (2022A1515010161), the Guangdong Basic and Applied Basic Research Foundation (2021B1515130008), and the National Natural Science Foundation of China (51977062).

Article history

Received: 9 July 2022; Revised: 28 July 2022; Accepted: 31 July 2022

Additional information

Supplementary information The online version contains supplementary material available at https://doi.org/10.23919/IEN.2022.0031.

Declaration of competing interest

The authors have no competing interests to declare that are relevant to the content of this article.

References

[1] Fotouhi, A., Auger, D. J., Propp, K., Longo, S., Wild, M. (2016). A review on electric vehicle battery modelling: From lithium-ion toward lithium–sulphur. *Renewable and Sustainable Energy Reviews*, 56: 1008–1021.

[2] Abada, S., Marlair, G., Lecocq, A., Petit, M., Sauvant-Moynot, V., Huet, F. (2016). Safety focused modeling of lithium-ion batteries: A review. *Journal of Power Sources*, 306: 178–192.

[3] Han, Z. B., Wang, Q. (2022). Recent progress on dielectric polymers and composites for capacitive energy storage. *iEnergy*, 1: 50–71.

[4] Liu, H., Cheng, X. B., Yan, C., Li, Z. H., Zhao, C. Z., Xiang, R., Yuan, H., Huang, J. Q., Kuzmina, E., Karaseva, E., et al. (2022). A perspective on energy chemistry of low-temperature lithium metal batteries. *iEnergy*, 1: 72–81.

[5] Wang, Q., Jiang, B., Li, B., Yan, Y. Y. (2016). A critical review of thermal management models and solutions of lithium-ion batteries for the development of pure electric vehicles. *Renewable and Sustainable Energy Reviews*, 64: 106–128.

[6] Deng, J., Bae, C., Marcicki, J., Masias, A., Miller, T. (2018). Safety modelling and testing of lithium-ion batteries in electrified vehicles. *Nature Energy*, 3: 261–266.

[7] Ren, D. S., Feng, X. N., Liu, L. S., Hsu, H., Lu, L. G., Wang, L., He, X. M., Ouyang, M. G. (2021). Investigating the relationship between internal short circuit and thermal runaway of lithium-ion batteries under thermal abuse condition. *Energy Storage Materials*, 34: 563–573.

[8] Jin, C. Y., Sun, Y. D., Wang, H. B., Lai, X., Wang, S. Y., Chen, S. Q., Rui, X. Y., Zheng, Y. J., Feng, X. N., Wang, H. W., et al. (2021). Model and experiments to investigate thermal runaway characterization of lithium-ion batteries induced by external heating method. *Journal of Power Sources*, 504: 230065.

[9] Chen, K., Wu, W. X., Yuan, F., Chen, L., Wang, S. F. (2019). Cooling efficiency improvement of air-cooled battery thermal management system through designing the flow pattern. *Energy*, 167: 781–790.

[10] Zhao, G., Wang, X. L., Negnevitsky, M., Zhang, H. Y. (2021). A review of air-cooling battery thermal management systems for electric and hybrid electric vehicles. *Journal of Power Sources*, 501: 230001.

[11] Wang, N. B., Li, C. B., Li, W., Chen, X. Z., Li, Y. S., Qi, D. F. (2021). Heat dissipation optimization for a serpentine liquid cooling battery thermal management system: An application of surrogate assisted approach. *Journal of Energy Storage*, 40: 102771.

[12] Akbarzadeh, M., Kalogiannis, T., Jaguemont, J., Jin, L., Behi, H., Karimi, D., Beheshti, H., van Mierlo, J., Berecibar, M. (2021). A comparative study between air cooling and liquid cooling thermal management systems for a high-energy lithium-ion battery module. *Applied Thermal Engineering*, 198: 117503.

[13] Jiang, Z. Y., Qu, Z. G. (2019). Lithium-ion battery thermal management using heat pipe and phase change material during discharge-charge cycle: A comprehensive numerical study. *Applied Energy*, 242: 378–392.

[14] Safdari, M., Ahmadi, R., Sadeghzadeh, S. (2020). Numerical investigation on PCM encapsulation shape used in the passive-active battery thermal management. *Energy*, 193: 116840.

[15] Youssef, R., Hosen, M. S., He, J. C., AL-Saadi, M., van Mierlo, J., Berecibar, M. (2022). Novel design optimization for passive cooling PCM assisted battery thermal management system in electric vehicles. *Case Studies in Thermal Engineering*, 32: 101896.

[16] Murali, G., Sravya, G. S. N., Jaya, J., Vamsi, V. N. (2021). A review on hybrid thermal management of battery packs and it's cooling performance by enhanced PCM. *Renewable and Sustainable Energy Reviews*, 150: 111513.

[17] Huang, Q. Q., Li, X. X., Zhang, G. Q., Wang, Y. Z., Deng, J., Wang, C. H., Chen, T. X. (2021). Pouch lithium battery with a passive thermal management system using form-stable and flexible composite phase change materials. *ACS Applied Energy Materials*, 4: 1978–1992.

[18] Thakur, A. K., Sathyamurthy, R., Saidur, R., Pandey, A. K., Sharshir, S. W., Christopher, S. (2021). A critical review of recent development in Li-ion battery cooling using advance phase change materials. *ECS Transactions*, 105: 411–418.

[19] Bai, K. H., Li, C. C., Xie, B. S., Zhang, D. Y., Lv, Y. F., Xiao, J. B., He, M. Z., Zeng, X. L., Zeng, J. L., Chen, J. (2022). Emerging PEG/VO_2 dual phase change materials for thermal energy storage. *Solar Energy Materials and Solar Cells*, 239: 111686.

[20] Yin, G. Z., Yang, X. M., Hobson, J., López, A. M., Wang, D. Y. (2022). Bio-based poly (glycerol-itaconic acid)/PEG/APP as form stable and flame-retardant phase change materials. *Composites Communications*, 30: 101057.

[21] Wei, P. R., Cipriani, C. E., Pentzer, E. B. (2021). Thermal energy regulation with 3D printed polymer-phase change material composites. *Matter*, 4: 1975–1989.

[22] Chen, X., Gao, H. Y., Tang, Z. D., Dong, W. J., Li, A., Wang, G.

(2020). Optimization strategies of composite phase change materials for thermal energy storage, transfer, conversion and utilization. *Energy & Environmental Science*, 13: 4498–4535.

[23] Xie, Y. H., Li, W. J., Huang, H. W., Dong, D. X., Zhang, X. Y., Zhang, L., Chen, Y., Sheng, X. X., Lu, X. (2020). Bio-based Radish@PDA/PEG sandwich composite with high efficiency solar thermal energy storage. *ACS Sustainable Chemistry & Engineering*, 8: 8448–8457.

[24] Min, P., Liu, J., Li, X. F., An, F., Liu, P. F., Shen, Y. X., Koratkar, N., Yu, Z. Z. (2018). Thermally conductive phase change composites featuring anisotropic graphene aerogels for real-time and fast-charging solar-thermal energy conversion. *Advanced Functional Materials*, 28: 1805365.

[25] Wang, Z. Y., Tong, Z., Ye, Q. X., Hu, H., Nie, X., Yan, C., Shang, W., Song, C. Y., Wu, J. B., Wang, J., et al. (2017). Dynamic tuning of optical absorbers for accelerated solar-thermal energy storage. *Nature Communications*, 8: 1478–1487.

[26] Qiu, J. C., Huo, D., Xia, Y. N. (2020). Phase-change materials for controlled release and related applications. *Advanced Materials*, 32: e2000660.

[27] Qiu, J. C., Huo, D., Xue, J. J., Zhu, G. H., Liu, H., Xia, Y. N. (2019). Encapsulation of a phase-change material in nanocapsules with a well-defined hole in the wall for the controlled release of drugs. *Angewandte Chemie International Edition*, 58: 10606–10611.

[28] Yu, D. H., He, Z. Z. (2019). Shape-remodeled macrocapsule of phase change materials for thermal energy storage and thermal management. *Applied Energy*, 247: 503–516.

[29] Sui, Y. L., Sima, H. F., Shao, W. D., Zhang, C. L. (2022). Novel bioderived cross-linked polyphosphazene microspheres decorated with FeCo-layered double hydroxide as an all-in-one intumescent flame retardant for epoxy resin. *Composites Part B: Engineering*, 229: 109463.

[30] Zhang, J. Y., Li, X. X., Zhang, G. Q., Wu, H. W., Rao, Z. H., Guo, J. W., Zhou, D. Q. (2020). Experimental investigation of the flame retardant and form-stable composite phase change materials for a power battery thermal management system. *Journal of Power Sources*, 480: 229116.

[31] Hajiali, F., Tajbakhsh, S., Marić, M. (2020). Thermal characteristics and flame retardance behavior of phosphoric acid-containing poly(methacrylates) synthesized by RAFT polymerization. *Materials Today Communications*, 25: 101618.

[32] Yang, S., Zhang, Q. X., Hu, Y. F. (2016). Synthesis of a novel flame retardant containing phosphorus, nitrogen and boron and its application in flame-retardant epoxy resin. *Polymer Degradation and Stability*, 133: 358–366.

[33] Hajibeygi, M., Mousavi, M., Shabanian, M., Vahabi, H. (2020). The effect of phosphorus based melamine-terephthaldehyde resin and Mg–Al layered double hydroxide on the thermal stability, flame retardancy and mechanical properties of polypropylene MgO composites. *Materials Today Communications*, 23: 100880.

[34] Wang, W., Pan, H. F., Shi, Y. Q., Pan, Y., Yang, W., Liew, K. M., Song, L., Hu, Y. (2016). Fabrication of LDH nanosheets on β-FeOOH rods and applications for improving the fire safety of epoxy resin. *Composites Part A: Applied Science and Manufacturing*, 80: 259–269.

[35] Yuan, H., Qian, X. D., Song, L., Lu, H. D. (2014). Polymer/layered compound nanocomposites: A way to improve fire safety of polymeric materials. *Fire Safety Science*, 11: 66–82.

[36] Zhang, H. J., Li, K., Wang, M. C., Zhang, J. F. (2021). The preparation of a composite flame retardant of layered double hydroxides and α-zirconium phosphate and its modification for epoxy resin. *Materials Today Communications*, 28: 102711.

[37] Yen, Y. Y., Wang, H. T., Guo, W. J. (2012). Synergistic flame retardant effect of metal hydroxide and nanoclay in EVA composites. *Polymer Degradation and Stability*, 97: 863–869.

[38] Lu, Y. H., Wu, C. F., Xu, S. A. (2018). Mechanical, thermal and flame retardant properties of magnesium hydroxide filled poly(vinyl chloride) composites: The effect of filler shape. *Composites Part A: Applied Science and Manufacturing*, 113: 1–11.

[39] Lyu, B., Wang, Y. F., Gao, D. G., Ma, J. Z., Li, Y. (2019). Intercalation of modified zanthoxylum bungeanum Maxin seed oil/stearate in layered double hydroxide: Toward flame retardant nanocomposites. *Journal of Environmental Management*, 238: 235–242.